

Study of Oxygen Deprived V307L Mutated Cardiac Ventricular Cell

¹Asjad Raza, ²Dr. Ch Srinivasulu, ³Dr. Ambati Rama Mohan Reddy, ⁴Dr. R.M. Noorullah

¹⁻⁴Institute of Aeronautical Engineering, Dundigal, Hyderabad-500043, India.

*Corresponding Author: Dr. R.M. Noorullah, E-mail: noorullah.rm@iare.ac.in

Cite this paper as: Asjad Raza, Dr. Ch Srinivasulu, Dr. Ambati Rama Mohan Reddy, Dr. R.M. Noorullah (2025), Study of Oxygen Deprived V307L Mutated Cardiac Ventricular Cell. *Frontiers in Health Informatics*, 14(2)2693-2704

ABSTRACT

Introduction: Arrhythmia is an irregular heartbeat. Arrhythmias occur when the electrical signals that coordinate the heartbeat do not work properly. Cardiac arrhythmia can develop as a result of tissue damage, medication exposure, or genetic mutation. Bradycardia and tachycardia are caused by poor signaling. Heart arrhythmias are often categorized according to how quickly the heart beats. The average heartbeat is between 70 and 80 beats per minute. The difference between tachycardia and bradycardia is the speed of the heartbeat. Some cardiac arrhythmias can be fatal. A person's heart rate might be rapid or sluggish, though, and that is normal. For instance, the heart rate may rise during physical activity or fall during sleep. Surgery, medical treatments, implanted devices, and anti-arrhythmic medications are all used in treatment. An analysis of the changes in output based on changes in input constitutes a computational study, which is essentially the modeling of a biological system as a set of differential equations. To comprehend the impact of oxygen deprivation in a cardiac ventricular cell with the V307L mutation, simulation research is conducted. The action potential duration is longer in cells with oxygen deprivation than it is in cells with the V307L mutation. The oxygen deprivation in V307L mutant cells was investigated under heterozygous, homozygous, and wild-type conditions. It has been found that the Action Potential Duration (APD) of oxygen-deprived heterozygous and homozygous cells is roughly 250 ms, leading us to draw the conclusion that, although oxygen deprivation causes a longer APD and the V307L mutation causes a shorter APD, the combination of the two causes Short QT Syndrome. The spike of the action potential shows a minor alteration.

Objectives: To Study the effect of V307L mutation in a cardiac ventricular cell, To Study the effect of oxygen deprivation in a cardiac ventricular cell, and To Study the effect of oxygen deprivation in V307L mutated cardiac ventricular cell.

Methods: The investigation, acquisition, and advancement of knowledge regarding physiological systems are made possible through mathematical modelling. As a result, modelling is an effective technique for gaining access to the oxygen deprived V307L cardiac ventricular cell. Additionally, using models to mimic various scenarios allows for the reconstruction of experiments and comparison of the results. The genetic mutation effect is simulated by adding the alterations to the slow delayed rectifier potassium current (IKs). In particular, the IKs expression was modified to take into consideration the experimental values of SQT2-linked KCNQ1 V 307 L mutation as noted by Bellocq et al. There are four mutation states of interest, viz. wild-type (WT).

Results: The percentage difference of the APD in wild-type (WT) and Het mutation is presented in Table II. The findings show that there is almost similar percentage of change in APD of M-cells when $\text{fac} = 0.6$ to that of the endocardial and epicardial cells. Nonetheless, the longer the fac value, the more the APD of M-cells extends. With the increase in APD, the absolute difference of APD decreases as well as the percentage change in a WT and Het case.

Conclusions: A computational study is carried out to understand the effect of oxygen deprivation in V307L mutated cardiac ventricular cell. In V307L mutated cell the action potential duration is shorter and in Oxygen deprived cell the action potential duration is longer. Heterozygous, homozygous and wild type conditions of V307L mutated cell were considered and oxygen deprivation in both the conditions of mutated cells were studied. It is observed that Action Potential Duration of oxygen deprived heterozygous and homozygous cells are approximately 250ms and so we may conclude that oxygen deprivation results in longer Action Potential Duration, V307L mutation gives shorter Action Potential Duration, Combination of both have Short QT Syndrome (SQTS) in Action Potential Duration when compared to the normal cells.

Keywords: *Arrhythmia, V307L, Mefloquine, QT interval, Short QT syndrome, Sudden Death*

INTRODUCTION

The heart is a very crucial muscle organ that functions to pump blood to all parts of the body through the circulatory system with the help of blood vessels. It is in such a transparent manner that oxygen and other nutrients are sent to body tissues, and waste substances like carbon dioxide are floated away to the respiratory organs to be expelled. The heart can sometimes fail to keep its normal rhythm. This abnormal or improper beating of the heart is what is described as arrhythmia, and this usually occurs as a result of disruptions to either the production or conduction of electrical signals. Myocardial ischemia is a condition arising as a result of insufficient supply to the heart muscle, owing to insufficient supply of oxygen to the body. This ailment is usually brought about by either partial or full blockages in the coronary arteries that hinder blood flow. This reduces the efficient pumping of the heart. This entails a total and abrupt interference with its functioning and can result in a heart attack; also slowing down of the blood flow causes another very serious case of arrhythmias. The risk factors include intense physical burden, heart disease, and foods that are high in cholesterol. A phospholipid bilayer membrane surrounds every cardiac cell. This membrane faces the extracellular space on its outside environment and the intracellular space on its inner side. Within the bilayer are special proteins acting as ion channels, which allow specific permeability to specific ions. Together with the ion pumps, these channels form ion gradients that generate a membrane potential difference, which is vital in the normal operation of the cardiac cells. The mechanism of cardiac cell depolarization starts with an influx of sodium ions (Na^+) into the intracellular space, which occurs under the action of the rapid opening of voltage-gated sodium channels in Phase 0 of the action potential. This is succeeded by a short repolarisation (Phase 1), which is affected by the outflow of potassium ion (K^+). During Phase 2, the plateau phase, there is an influx of calcium ions (Ca^{2+}) into the cell, and the balance between this and potassium ions efflux leads to membrane potential stability being maintained over time. The cessation of the calcium entry leads to the dominance of the sustained potassium efflux, resulting in additional repolarization (Phase 3). Phase 4 lastly, the cell processes back to the normal membrane electrical position, restoring the resting membrane potential. This project aims to develop a robust predictive framework for cardiovascular disease using various data mining techniques and to systematically compare their performance based on evaluation metrics such as accuracy, sensitivity (true positive rate), and specificity (true negative rate). The research is guided by two primary objectives: first, to propose an effective prediction model that can assess the risk of heart disease using patient data, and second, to evaluate the potential benefits of ensemble learning—combining multiple models—to achieve greater reductive accuracy and reliability compared to single-model approaches. Through this study, we aim to contribute toward improving the precision of cardiovascular diagnostics and supporting healthcare professionals in making informed decisions for patient care.

Electrical activity of the heart and Conduction system of the heart

The human heart is a remarkable organ known for its **autorhythmicity**, a property that allows it to generate and regulate its own rhythmic contractions without requiring external nervous stimulation. This self-initiated electrical activity is made possible by **specialized cardiac muscle cells** that form the heart's intrinsic conduction system. These specialized cells are not typical contractile muscle fibers; instead, they are capable of spontaneously generating **action potentials** that set the pace for the heart's rhythm.

"Figure 1" provides a detailed cross-sectional view of the human heart, clearly highlighting the components of the conduction system, which are marked in green for emphasis. This conduction system coordinates the electrical impulses that ensure the heart's four chambers contract in a synchronized and efficient manner, thereby maintaining effective blood circulation throughout the body.

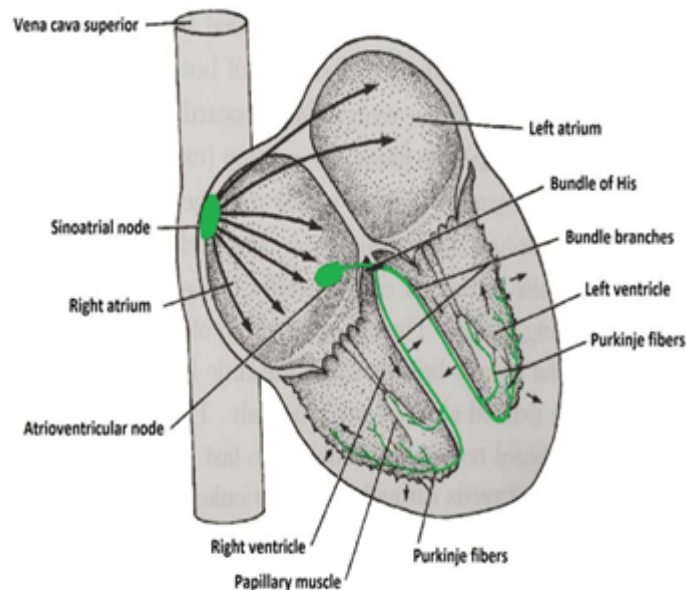


Figure 1: Cross-sectional View of Human Heart

Cardiac action potential

The **cell membrane** of every **cardiac muscle cell (cardiomyocyte)** is composed of a **phospholipid bilayer**, which forms a dynamic and selectively permeable barrier between the internal and external environments of the cell. This bilayer is structurally organized with hydrophilic phosphate heads facing outward and hydrophobic lipid tails directed inward, creating a stable configuration that isolates the **intracellular space** (inside the cell) from the **extracellular space** (outside the cell). Embedded within this lipid matrix are a variety of **membrane proteins**, many of which play critical roles in maintaining cellular homeostasis and facilitating the electrical activity that drives cardiac contraction.

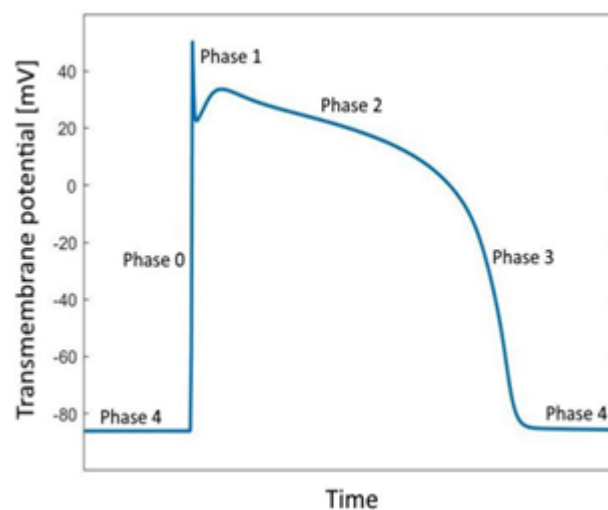


Figure 2: Representation of ionic gradients

“Figure 2” provides a schematic representation of these ionic gradients and the forces that influence ion movement across the membrane. Two key forces regulate this **ion flow**:

1. **Chemical (Concentration) Gradient:** This refers to the natural tendency of ions to move from regions of **high**

concentration to low concentration. For example, Na^+ will move into the cell where its concentration is lower, while K^+ tends to move out of the cell.

2. **Electrical Gradient:** Because ions carry charge, their movement also generates and responds to electrical fields. Positively charged ions are attracted to negatively charged areas and repelled by positively charged regions.

The **balance between these two forces** for a given ion results in an **equilibrium potential**, also known as the **Nernst potential**. This is the membrane voltage at which there is no net movement of that specific ion across the membrane. For potassium (K^+), this potential is typically around **-86 mV**, which closely corresponds to the **resting membrane potential** of a cardiac cell.

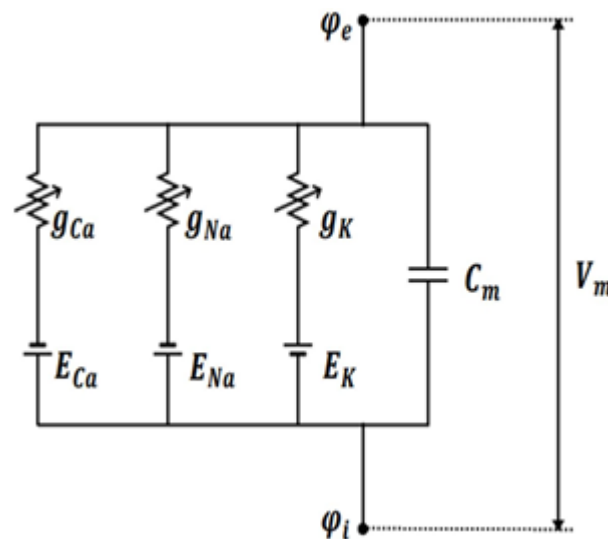


Figure 3: Description of Membrane Voltage

When a stimulus is strong enough to **depolarize the membrane** beyond a certain **threshold potential**, an **action potential** is initiated. This is a rapid, transient change in membrane voltage that occurs in distinct phases, as shown in “Figure 3”.

The **action potential** in cardiac cells proceeds through the following phases:

- **Phase 0 (Depolarization):** Triggered by a rapid influx of Na^+ ions through **voltage-gated sodium channels**, causing a sharp rise in membrane potential. This is the initial upstroke of the action potential.
- **Phase 1 (Initial Repolarization):** A brief **efflux of K^+ ions** begins through specific potassium channels, slightly decreasing the membrane potential.
- **Phase 2 (Plateau Phase):** Unique to cardiac cells, this phase involves a delicate balance between Ca^{2+} **influx** through L-type calcium channels and continued K^+ efflux. This plateau is critical for prolonging the refractory period and preventing premature contractions.
- **Phase 3 (Repolarization):** As Ca^{2+} **channels close**, continued K^+ **efflux** restores the membrane potential toward the resting level.
- **Phase 4 (Resting Phase):** The **resting membrane potential** is maintained, primarily by the Na^+/K^+ **pump** and K^+ leak channels, until the next action potential is initiated.

MOTIVATION

Analyze the effects of arrhythmias in humans and develop appropriate treatment models to help in better visualization

NOVELTY

The Action Potential Duration of oxygen deprived heterozygous and homozygous V307L cardiac ventricular cell is modeled, observed and studied.

LITERATURE SURVEY

The Hodgkin-Huxley (HH) model was first conceived to describe that process in the squid giant axon. The membrane potential of this model is mostly determined by the membrane potential at rest or oscillation in response to outside stimuli or applied currents. A neuron can generate an action potential when depolarization and repolarization processes take place in an orderly fashion. Such dynamics are defined by the likelihood of opening or closing of gates in the ion channels, which further determines the movement of these ions across the cell membrane. Classical HH formulation models the potassium (K^+) current as having various activation gates, which causes the gating variable, as a power of four. Nevertheless, variants of the HH model have tested higher degrees of potassium activation (e.g., 5 or 6), and such can be compared to the original formulation. The findings demonstrate that the modified models with more advanced activation of potassium recover to resting faster in high external current and stabilize after oscillatory behaviour. Interestingly, variation in Hopf bifurcation points indicates that the qualitative behaviours of the revised models depart deeply from the classical HH model. Ostensibly, the HH model beautifully described the mechanisms behind excitation in neurons. More than its technical value, however, the novelty and rigor of their quantitative approach is one of the most influential papers in neuroscience, establishing the field of modern computational and theoretical neurobiology. The negative modulation of gap junctional conductance (GJC) between the endocardial and mid-myocardial sections of the heart affects the conduction of the action potentials. Mid-myocardial layer (M-cells) has been reported to have the long action potential durations (APD) compared cells. The pacing site, as depicted in the simulation setting, entails a small group of cells (cells 1:2 or 1:10) presented at the inner corner or lower-left of the tissue being triggered at an interval of 800ms. These dynamics are represented using normalized pseudo-ECGs produced using the mathematical models of Gima et al.

Beeler - Reuter Model: The first ventricular model was published by Beeler and Reuter in 1977. This model uses four of the eight different ionic currents known at the time in cardiac muscle. They implemented a fast inward Na^+ current I_{Na} , similar to the one used by Hodgkin and Huxley, but they added a second slower inactivation gate j , the time-dependent outward current I_{K1} , a time-independent K^+ outward current I_{K1} , and a slow inward current I_s carried primarily by Ca^{2+} . The total ionic current in the Beeler-Reuter model is given by four currents, and the model uses eight variables. Courtemanche and Winfree used the Beeler-Reuter model to simulate the first ionic model in 2D. (1991). It not only revealed for the first time that ionic models could generate spiral waves, but also that they could split into many waves (see Figure 10). Breakup in this model is caused by delayed recovering fronts (Courtemanche, 1996). Breakup can be avoided by increasing the speed of the calcium dynamics, which decreases the huge variation in wavelengths.

Ten Tusscher Model: A human ventricular tissue model. There are few experimental and clinical options for researching cardiac arrhythmias in human ventricular myocardium. As a result, the utilisation of alternative methodologies such as computer simulations is critical. In this paper, we present a mathematical model of the action potential of human ventricular cells that, although including a high degree of electrophysiological information, is computationally cheap enough to be used in large-scale spatial simulations for the investigation of reentrant arrhythmias. The model is based on new experimental data on the majority of the main ionic currents, including fast sodium, L-type calcium, transient outward, quick and slow delayed rectifier, and inward rectifier currents. The genetic mutation effect is simulated by adding the alterations to the slow delayed rectifier potassium current (IKs). In particular, the IKs expression was modified to take into consideration the experimental values of SQT2-linked KCNQ1 V 307 L mutation as noted by Bellocq et al. There are four mutation states of interest, viz. wild-type (WT).

OBJECTIVES

1. To Study the effect of V307L mutation in a cardiac ventricular cell.
2. To Study the effect of oxygen deprivation in a cardiac ventricular cell.
3. To Study the effect of oxygen deprivation in V307L mutated cardiac ventricular cell.

The investigation, acquisition, and advancement of knowledge regarding physiological systems are made possible through mathematical modelling. As a result, modelling is an effective technique for gaining access to the oxygen deprived V307L cardiac ventricular cell. Additionally, using models to mimic various scenarios allows for the reconstruction of experiments and comparison of the results.

METHODS

Equations used for V307L mutated cardiac ventricular cell:

$$I_{Ks} = G_{Ks} x_s^2 (V_m - E_K) \quad -1$$

$$\alpha_{xs} = 1400(1 - e^{(5 - V_m)})/6 \quad -2$$

$$\beta_{xs} = 1/(1 + e^{(V_m - 35)/15}) \quad -3$$

$$x_{sco} = 1/(1 + e^{(-5.9 - V_m)/17.4}) \quad -4$$

$$T_{xs} = (\alpha_{xs} \beta_{xs} + 80) \quad -5$$

$$x_{sco} = 1/(1 + e^{(-20.62 - V_m)/10.96}) \quad -6$$

$$x_{sco} = 1/(1 + e^{(-24.05 - V_m)/16.09}) \quad -7$$

$$T_{xs} = 0.7(\alpha_{xs} \beta_{xs} + 80) \quad -8$$

$$T_{xs} = 0.52(\alpha_{xs} \beta_{xs} + 80) \quad -9$$

In order to study the degree of action potential duration (APD) shortening in M-cells that predispose to arrhythmia and the heterozygous SQT2 mutation is introduced to the cardiac model. Common premature beats are used in the pacing sequence to determine if the ability to stimulate arrhythmogenic events is possible under this genetic condition. Such a strategy enables testing the susceptibility of M-cells with shortened APD to reentrant conduction and aberrancies and, by extension, brings insights regarding the arrhythmogenic capabilities of SQT2.

Table 1: Description of Scaling Factor values of various cells in various mutations

	Scaling Factors M-Cells	Scaling Factor of Endo/Epi Cells
Wild Type	1.0000	1.0000
Heterozygous	0.7500	0.7000
Homozygous	0.5800	0.5200
Homozygous-Reduced	0.3800	0.3200

All the cells of the simulated cardiac tissue could be paced at a nominal heart rate of 75 beats per minute, and SQT2 gene mutations could be randomly introduced in every cell. The wavefront spreads upwards as the tissue is electrically stimulated by the conduction upwards with the shape of a convex depolarization. This explains why the stimulation process occurs sequentially via the endocardial, mid-myocardial (M), and epicardial layers. During conduction, the endocardial cells and epicardial cells are depolarized concomitantly, though the M-cells would always form the lagging end. Such a layering-activating profile generates clear differences in the pseudo-ECG signal. One can explain a positive T-wave in the pseudo-ECG by differences in timings of repolarization of the three layers. Quantitative measures, such as QT_{dur}, T-peak, and T_{dr}- transmural dispersion of repolarization of each genetic condition are delineated as shown in Table II. The difference between T-peak and T-end gives the TDR, which gives a direct expression of the heterogeneity of the repolarization within the wall of the ventricle. The analysis shows that with the increase in the mutation (wild-type mutation to Hom to HomRed), the QT intervals decrease, whereas the values of T-peak and TDR increase. According to these observations, it can be stated that changes in the channel kinetics of I_{Ks} based on genetic modifications have an important effect on the heterogeneity of ventricular repolarization. As a result of this, this will directly implicate the changes that can be observed as abnormal T-wave morphology, as is present in Short QT Syndrome type 2 (SQT2) APD in single Cells: All three

cardiac cell types (endocardial, mid-myocardial (M) and epicardial) They are targeted with the SQTS2 heterozygous (Het) mutation injected in, and the resulting action potential duration (APD) is calculated. In endocardial and epicardial cells, the scaling factor (fac) is set at 0.7. Conversely, in the case of M-cells, five values of fac are considered; i.e., 0.6, 0.65, 0.7, 0.75, and 0.8.

RESULTS AND DISCUSSION

The percentage difference of the APD in wild-type (WT) and Het mutation is presented in Table II. The findings show that there is almost similar percentage of change in APD of M-cells when $\text{fac} = 0.6$ to that of the endocardial and epicardial cells. Nonetheless, the longer the fac value, the more the APD of M-cells extends. With the increase in APD, the absolute difference of APD decreases as well as the percentage change in a WT and Het case.

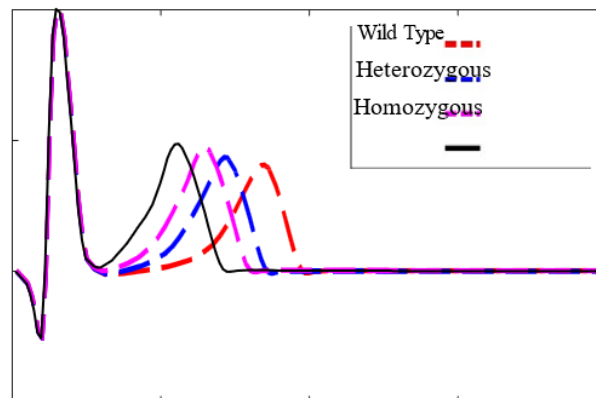


Figure 4: Description of Pseudo ECG for genetic mutation

Table 2: Description of Short QT Syndrome type 2 (SQTS2) parameters

Gene Mutation	QT interval (ms)	Tpeak (mV)	TDR (ms)
Wild Type	350	0.4038	50
Heterozygous	300	0.4350	55
Homozygous	275	0.4716	60
Homozygous-Reduced	245	0.4856	65

SQTS2 conditions were recreated by measuring action potential duration (APD) of cells in WT and the mutation and measuring the change in ADP. In spite of previous research reports which showed the differences in APD between Het and WT states, they did not actually quantify the percent change. Upon calculation, the decrease of APD was observed to be 28.31, 21.65 and 28.59 in epicardial, mid-myocardial and endocardial cell respectively. These values support the results of the current investigation, which points out that the APD variability of M-cells continues to be about 5 -7 percent less than that of endocardial and epicardial cells. This differential promotes formation of reentrant wavefronts both in the two- and three-dimensional tissue model.

Table 3: Description of Short QT Syndrome type 2 (SQTS2) parameters

	APD in WT (ms)	APD in Het (ms)	fac	Delta APD (ms)	% Change in APD
Endo Cardinal	281.80	225.45	0.75	56.45	20.00
Epi Cardinal	251.95	198.25	0.75	53.75	21.30
M-Cell	362.60	288.88	0.65	73.85	20.35
		296.65	0.65	66.65	18.25
		303.96	0.73	58.75	16.85
		310.78	0.75	51.96	14.35
		317.15	0.85	45.55	12.75

The outcomes also show that reentrant steady-state is maintained to a greater duration when within 5-7 percent range, the decrease in APD through WT and Het mutations is less. On the other hand, when the proportionate level of M-cell loss is close to the level of elimination of endocardial or epicardial cells, reentrant waves do not transfer, which explains the significance of the relative variation in APDs as a means of arrhythmias beginning.

Nonetheless, there are limitations of the study. The model has a simplified geometry where the whole mid-myocardial layer is composed of M-cells when they in fact tend to form clusters in experimental trials as island like structures, rather than continuous layer. In addition, there is no extensive study that compares the percentage changes in ADP between M-cells and other cell types particularly under WT and Het conditions. Other genetic variations including homozygous (Hom) and homozygous reduced (HomRed) should be used as well in future studies to give full view of the manifestations of SQTS2. Moreover, the possible therapeutic effect of such agents as quinidine and their influence on the APD shortening of endocardial, mid-myocardial and epicardial cells should be studied in a systematic way to define the potential applicability in the clinical practice of SQTS2. At 4.285 s, when the first premature beat (PB) takes place, the middle-myocardial (M) cells have not been repolarized already. Consequently, the resulting wavefront propagates along the endocardial layer and enters mid-myocardial and epicardial areas at the top of the tissue and a representation of it is depicted in Fig. 6(ii)(b). Then the wavefront propagates down the epicardial layer and then reenters through the mid and endocardial layers again (Fig. 6(ii)(c)). Such a sequence leads to the formation of a reentrant wave, which keeps circulating as shown in Fig. 6(ii)(d-g), until every cell again reaches a resting state shortly before the implementation of the third PB at 4.81 s (Fig. 6(ii)(h)). A regular rhythm is then reestablished with a normal sequence of depolarization and repolarization at 5.6 s generated by the third PB.

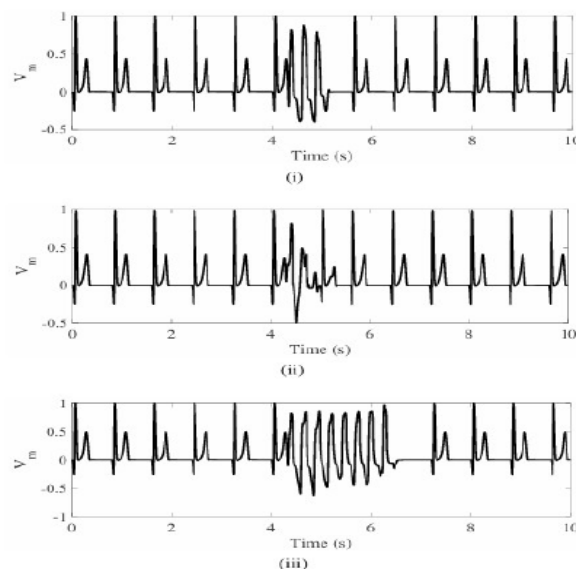


Figure 5: Description of the pseudo-ECG generated when ‘fac’ in M-Cell (i) 0.6, (ii) 0.7, and (iii) 0.75

Simultaneously, the Fig. 5(iii) presents the pseudo- ECG reaction using the same pacing protocol only at a tenfold larger value of the scaling factor (fac) = 0.75. Three consecutive PBs yield the appearance of an arrhythmia-like pattern, which is however not maintained, with the normal rhythm eventually returning again after a lengthy delay. Within such a framework, M-cell APD is shorter than endocardial or epicardial cell APD, by around 5-7% of the endocardial or epicardial cell, a disparity that is compatible with electrophysiological conditions that promote the generation of reentrant waves. Also, with $\text{fac} = 0.8$, only one PB is needed to get the reentrant activity started. These reentrant waves continue after administration of both the second and the third PBs, although by 5.37 s all cells have repolarised. Normal rhythm is restored by the pacing stimulus again in 5.6 s contravening the right ventricle to create the usual QRS complex (not pictured). Generation of Arrhythmia: A regular pacing of the tissue is done at 800 ms. Three premature beats (PBs) (cycle length 270ms) in the form of three premature beats are applied after six standard

pacing pulses in order to assess the possibility of arrhythmia generation. The associated pseudo- ECGs under these protocol as well as in respect to the variation in scaling factor ($\text{fac} = 0.6, 0.65, 0.7, 0.75$ and 0.8) are demonstrated in the in the figure 5.

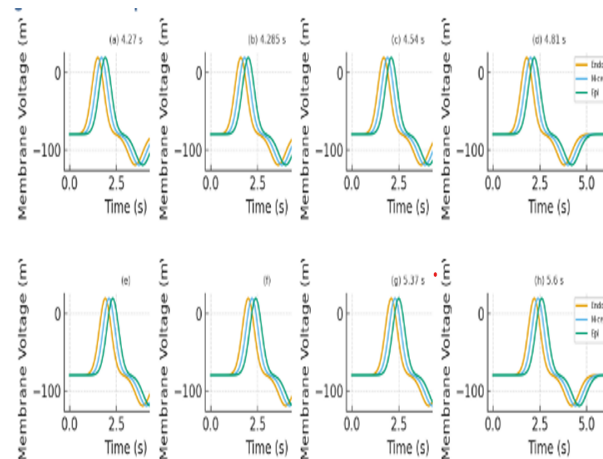


Figure 6: Line graph representation of action potentials in Endocardial, Mid-myocardial and Epicardial cells

The voltage snapshots of the tissue that treatments the first PB were taken at 4.27 s are depicted in Figure. 6(i)(a). The M-cells at this moment are still in repolarizing. As a result, the wave of depolarization is moving upwards via the endocardial layer and further diffusing into the mid-myocardial and epicardial area (Figure. 6(i)(b)). The last to repolarize is the cells at the upper mid and epicardial layers. This trending tendency can be remembered in the second and third PBs that were used at 4.54 s and 4.81 s, respectively Figure 6(i) (c-h). The resulting pseudo- ECGs exhibit an inverted T-wave morphology but they do not generate sustained reentry. At $\text{fac} = 0.65$, with the same pacing protocol, wave activity in the reentrant wave form is established after the second PB and it is still present even after the third PB. Nonetheless, at 5.6 s all the cells are synchronized in depolarization, and the normal pacing frequency starts again (not shown). The first PB has a pseudo-ECG pattern at $\text{fac} = 0.7$ involving an upward-upward complex (Figure 5(ii)). The third PB with the value of 4.81 s, a positive T-wave is observed in the QRS complex, but the amplitude is not so clear in this case. The normal QRS complexes are replaced after 5.6 s. The related tissue-voltage maps of that proposition are in Figure 6(ii) (a). 4.285 s first PB. The wavefront caused by the PB will travel up the endo in the quiescent layer of cells and then right into the mid and epi layer at the top of tissue as seen in Figure 6(ii)(b) since the mid cells are still repolarizing. This wave traverses in a downward direction on epi layer and once again enters to the mid and endo layer as observed in Figure 6(ii) (c). This reentrant wave proceeds in Figure 6(ii) (d-g) whereby all the cells are back at rest state barely before and third PB is applied after 4.81 s in Figure 6(ii) (h). The third PB induces the normal repolarization and depolarization and normal rhythm reemerges at 5.6 s displays the pseudo ECG under application of the same pacing protocol and increasing the fac into 0.75. The maximum likelihood estimation is normally used to estimate the regression coefficients. The maximum likelihood ratio assists in knowing whether the independent variables have significant effects on the dependent variables statistically. The likelihood ratio test provides an evaluation of the effect of single predictors (independent variables). Thereafter, odds ratio is further used to calculate the probability (p) of each case. On the basis of this p-value, it is determined. This provides the possibility or the likelihood of the person having a coronary heart condition.

Objective 1 Results: Action potential durations of V307L mutated cardiac ventricular cell are in 3 types, they are Wild type, Heterozygous and Homozygous mutations

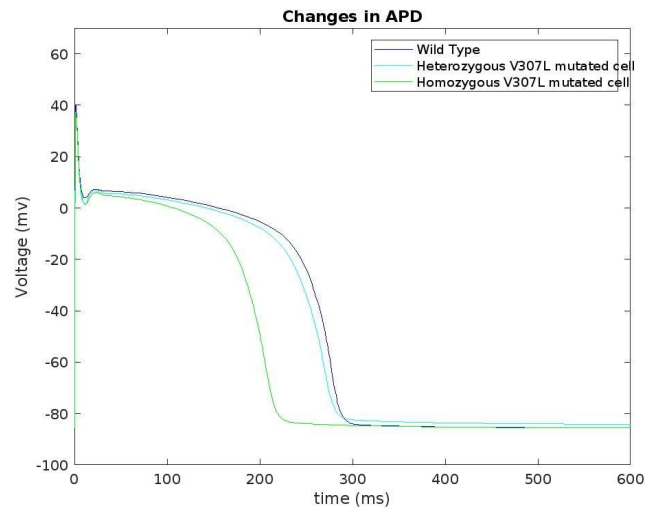


Figure 7: Description of Action potential durations of V307L mutated cardiac ventricular cell

Objective 2 Results: Action potential duration of oxygen deprived cardiac ventricular cell is studied

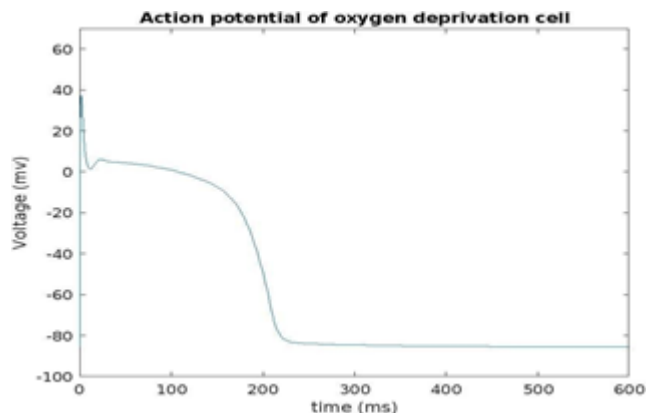


Figure 8: Description of Action potential duration of oxygen deprived cardiac ventricular cell

Objective 3 Results: Action potential durations of wild type, homozygous and heterozygous V307L mutated cells are plotted along with oxygen deprived normal cardiac ventricular cell, heterozygous and homozygous mutated cells are plotted and studied.

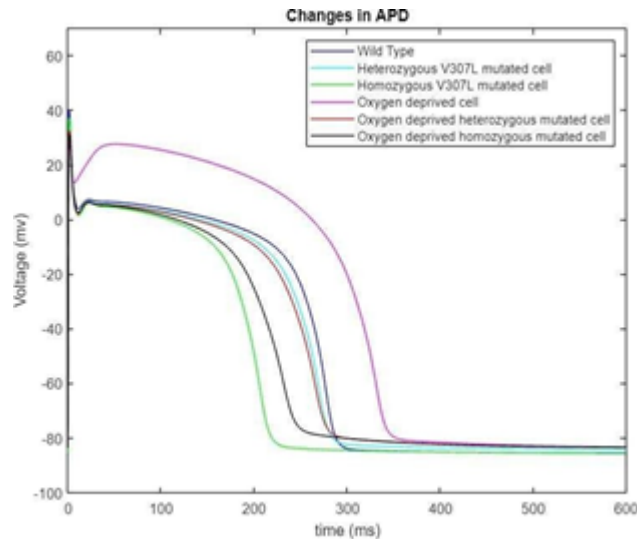


Figure 9: Description of Action potential durations of wild type, homozygous and heterozygous V307L mutated cells

CONCLUSION

A computational study is carried out to understand the effect of oxygen deprivation in V307L mutated cardiac ventricular cell. In V307L mutated cell the action potential duration is shorter and in Oxygen deprived cell the action potential duration is longer. Heterozygous, homozygous and wild type conditions of V307L mutated cell were considered and oxygen deprivation in both the conditions of mutated cells were studied. It is observed that Action Potential Duration of oxygen deprived heterozygous and homozygous cells are approximately 250ms and so we may conclude that oxygen deprivation results in longer Action Potential Duration, V307L mutation gives shorter Action Potential Duration, Combination of both have Short QT Syndrome (SQTS) in Action Potential Duration when compared to the normal cells.

ACKNOWLEDGEMENTS

This study was conducted without any external financial support. The authors confirm that there are no conflicts of interest. They also thank all reviewers for their valuable feedback, which has helped to improve this work.

REFERENCES

- [1] Mackay, J., Mensah, G. 2004 "Atlas of Heart Disease and Stroke" Nonserial Publication, ISBN-13 9789241562768 ISBN-10 9241562765.
- [2] Robert Detrano 1989 "Cleveland Heart Disease Database" V.A. Medical Center, Long Beach and Cleveland Clinic Foundation.
- [3] Yanwei Xing, Jie Wang and Zhihong Zhao Yonghong Gao 2007 "Combination data mining methods with new medical data to predicting outcome of Coronary Heart Disease" Convergence Information Technology, 2007. International Conference November 2007, pp 868-872.
- [4] Jianxin Chen, Guangcheng Xi, Yanwei Xing, Jing Chen, and Jie Wang 2007 "Predicting Syndrome by NEI Specifications: A Comparison of Five Data Mining Algorithms in Coronary Heart Disease" Life System Modeling and Simulation Lecture Notes in Computer Science, pp 129-135.
- [5] Jyoti Soni, Ujma Ansari, Dipesh Sharma 2011 "Predictive Data Mining for Medical Diagnosis: An Overview of Heart Disease Prediction" International Journal of Computer Applications, doi 10.5120/2237-2860.
- [6] Mai Shouman, Tim Turner, Rob Stocker 2012 "Using Data Mining Techniques In Heart Disease Diagnoses And Treatment" Electronics, Communications and Computers (JECECC), 2012 Japan-Egypt Conference March 2012, pp 173-17.
- [7] Dr. R.M. Noorullah, Dr. Shaik Ruksana Begam, Dr. Depruru Shobha Rani, Solapuram Shreeya (2024), Medi Molecule: An AI-Powered Platform for Accelerating Drug Discovery through Molecule Generation and Real-Time Collaboration. Frontiers in HealthInformatics, 14(2) 2534-2544.

- [8] K. H. ten Tusscher, D. Noble, P.-J. Noble, and A. V. Panfilov, "A model for human ventricular tissue," *American Journal of Physiology Heart Circulatory Physiology*, vol. 286, pp. H1573-H1589, 2004.
- [9] U. Saraswathi, Dr. R.M. Noorullah, Dr. Ambati Rama Mohan Reddy(2024), A Machine Learning Approach Using Statistical Models for Early Detection of Cardiac Arrest in Newborn Babies in the Cardiac Intensive Care Unit. *Frontiers in HealthInformatics*, 14(2) 2560-2574.
- [10] W. N. Wan Ab Naim, M. J. Mohamed Mokhtarudin, E. Lim, B. T. Chan, A. Ahmad Bakir, and N. A. Nik Mohamed, "The study of border zone formation in ischemic heart using electro-chemical coupled computational model," *International Journal for Numerical Methods in Biomedical Engineering*, vol. pp. e3398, 2020.